REPORT NO. NADC-89037-60

FATIGUE BEHAVIOR OF SILICON CARBIDE WHISKER/ALUMINUM COMPOSITE

Eun E. Lee
Air Vehicle and Crew Systems Technology Department (Code 6063)
NAVAL AIR DEVELOPMENT CENTER
Warminster, PA 18974-5000

1 OCTOBER 1988

FINAL REPORT
Task No. AP-8

Approved for Public Release; Distribution is Unlimited

Prepared for
NAVAL AIR DEVELOPMENT CENTER (Code 606)
Warminster, PA 18974-5000

NOTICES

REPORT NUMBERING SYSTEM - The numbering of technical project reports issued by the Naval Air Development Center is arranged for specific identification purposes. Each number consists of the Center acronym, the calendar year in which the number was assigned, the sequence number of the report within the specific calendar year, and the official 2-digit correspondence code of the Command Officer or the Functional Department responsible for the report. For example: Report No. NADC 88020-60 indicates the twentieth Center report for the year 1988 and prepared by the Air Vehicle and Crew Systems Technology Department. The numerical codes are as follows:

CODE	OFFICE OR DEPARTMENT
00	Commander, Naval Air Development Center
01	Technical Director, Naval Air Development Center
05	Computer Department
10	AntiSubmarine Warfare Systems Department
20	Tactical Air Systems Department
30	Warfare Systems Analysis Department
40	Communication Navigation Technology Department
50	Mission Avionics Technology Department
60	Air Vehicle & Crew Systems Technology Department
70	Systems & Software Technology Department
80	Engineering Support Group
90	Test & Evaluation Group

PRODUCT ENDORSEMENT - The discussion or instructions concerning commercial products herein do not constitute an endorsement by the Government nor do they convey or imply the license or right to use such products.

APPROVED BY: *William F. Moroney* DATE: *18 Aug 1989*

[illegible] MORONEY
[illegible] NAVY

Unclassified

SECURITY CLASSIFICATION OF THIS PAGE

REPORT DOCUMENTATION PAGE

Form Approved
OMB No 0704 0188

1a REPORT SECURITY CLASSIFICATION: Unclassified

1b RESTRICTIVE MARKINGS:

2a SECURITY CLASSIFICATION AUTHORITY:

2b DECLASSIFICATION / DOWNGRADING SCHEDULE:

3 DISTRIBUTION / AVAILABILITY OF REPORT: Approved for Public Release. Distributions is Unlimited

4 PERFORMING ORGANIZATION REPORT NUMBER(S): NADC-89037-60

5 MONITORING ORGANIZATION REPORT NUMBER(S):

6a NAME OF PERFORMING ORGANIZATION: Air Vehicle and Crew Systems Technology Department

6b OFFICE SYMBOL (If applicable): 6063

7a NAME OF MONITORING ORGANIZATION:

6c ADDRESS (City, State, and ZIP Code): NAVAL AIR DEVELOPMENT CENTER, Warminster, PA 18974-5000

7b ADDRESS (City, State, and ZIP Code):

8a NAME OF FUNDING / SPONSORING ORGANIZATION: Air Vehicle and Crew Systems Technology Department

8b OFFICE SYMBOL (If applicable): 60C2

9 PROCUREMENT INSTRUMENT IDENTIFICATION NUMBER:

8c ADDRESS (City, State, and ZIP Code): NAVAL AIR DEVELOPMENT CENTER, Warminster, PA 18974-5000

10 SOURCE OF FUNDING NUMBERS

PROGRAM ELEMENT NO	PROJECT NO	TASK NO	WORK UNIT ACCESSION NO
		AP-8	

11 TITLE (Include Security Classification): Fatigue Behavior of Silicon Carbide Whisker/Aluminum Composite

12 PERSONAL AUTHOR(S): Eun U. Lee

13a TYPE OF REPORT	13b TIME COVERED	14 DATE OF REPORT (Year, Month, Day)	15 PAGE COUNT
Final	FROM ______ TO ______	1988 October 1	22

16 SUPPLEMENTARY NOTATION:
Fatigue Behavior; Composite; Fratograph; Silicon Carbide Whisker; Constant Amplitude Loading; Micrograph

17 COSATI CODES

FIELD	GROUP	SUB-GROUP

18 SUBJECT TERMS (Continue on reverse if necessary and identify by block number):

19 ABSTRACT (Continue on reverse if necessary and identify by block number)

Specimens of an extruded 19.8 vol % SiCw/2124 aluminum alloy composite were subjected to constant amplitude loading of stress ratio 0.1 at room temperature in a laboratory atmosphere. The fatigue crack growth path is tortuous and much of it is nearly parallel to the extrusion direction of the specimen. This is attributable to the SiCw aligned in the extrusion direction. The logarithm of fatigue fracture life, N_f, increases linearly with decreasing stress range, $\Delta\sigma$, within the limits of the applied stress range. The relationship is defined by the equation: $\log N_f = 8.81 - \frac{\Delta\sigma}{115.7}$. The observed fractographic features are facets and steps in the initial stage, striations in the subsequent stage, and dimples in the final stage of fatigue.

20 DISTRIBUTION / AVAILABILITY OF ABSTRACT: ☒ UNCLASSIFIED/UNLIMITED ☐ SAME AS RPT ☐ DTIC USERS

21 ABSTRACT SECURITY CLASSIFICATION: Unclassified

22a NAME OF RESPONSIBLE INDIVIDUAL: Eun U. Lee

22b TELEPHONE (Include Area Code): 215-441-1663

22c OFFICE SYMBOL: 6063

DD Form 1473, JUN 86 — Previous editions are obsolete

S/N 0102-LF-014-6603

SECURITY CLASSIFICATION OF THIS PAGE
Unclassified

CONTENTS

FIGURES

ACKNOWLEDGEMENTS

This research was supported by the Office of Naval Technology through the Naval Air Development Center.

The author is grateful to Mrs. M. Donnellan for helpful discussions, Mr. R. Kowalik for fatigue testing, and Mr. W. Weist for his SEM work.

THIS PAGE INTENTIONALLY LEFT BLANK

INTRODUCTION

Metal matrix composites (MMC) of aluminum alloys reinforced with whisker or particulate silicon carbide have been studied extensively in recent years[1-23]. These composites have a high specific modulus and strength, low coefficient of thermal expansion, and good thermal stability[15-20]. In contrast to continuous filament MMC, they can offer isotropic properties, easier fabricability and formability, and potentially low cost. However, like continuous filament MMC, their ductility and fracture toughness are low,[8,15,21-23] they fail in a relatively brittle manner, and their fatigue behavior is not well characterized or understood. The increasing number of applications of SiC/Al composites in aero-vehicles demands a detailed knowledge of their fatigue behavior. The objective of this study is to characterize the fatigue behavior of a silicon carbide whisker reinforced aluminum matrix composite.

THIS PAGE INTENTIONALLY LEFT BLANK

EXPERIMENTAL PROCEDURE

The experimental procedure includes Material and Specimen Preparation, Tension and Fatigue Testing, and Microstructural and Fractographic Examination.

MATERIAL AND SPECIMEN PREPARATION

The specimen material was a silicon carbide whisker reinforced aluminum matrix composite, designated SXA24E/20W-T8E510 (19.8 vol % SiCw/Al-3.7 Cu-1.4 Mg), fabricated by Advanced Composite Materials Corp., Greer, SC. This material was initially double extruded from a 12 in. dia billet to a 4 in. dia. rod, machined to a 3 in. dia. billet, extruded to 0.25 in. x 1.5 in. bar, stretched after solution annealing and cold water quenching, and aged for 10 hours at 320°F. From this material, rectangular tension test and center-cracked-tension specimens were machined, as shown in Figure 1

TENSION AND FATIGUE TESTS

The tension and fatigue tests were conducted at room temperature in a laboratory atmosphere using a closed-loop electro-hydraulic MTS machine. During the tension test, the loading rate was 5,200 lb/min. The fatigue test conditions were stress ratio ($\sigma_{min}/\sigma_{max}$) of 0.1, constant amplitude loading of a haversine waveform, and a frequency of 10 Hz.

MICROSTRUCTURAL AND FRACTOGRAPHIC EXAMINATION

The specimen planes, perpendicular and parallel to the extrusion direction, were polished, etched by Keller's reagent, and examined in an Advanced Metals Research 1000 scanning electron microscope, operated at an accelerating voltage of 20 kV. The fractographic examination of tension-fractured and fatigue-fractured specimens was also carried out using the same scanning electron microscope.

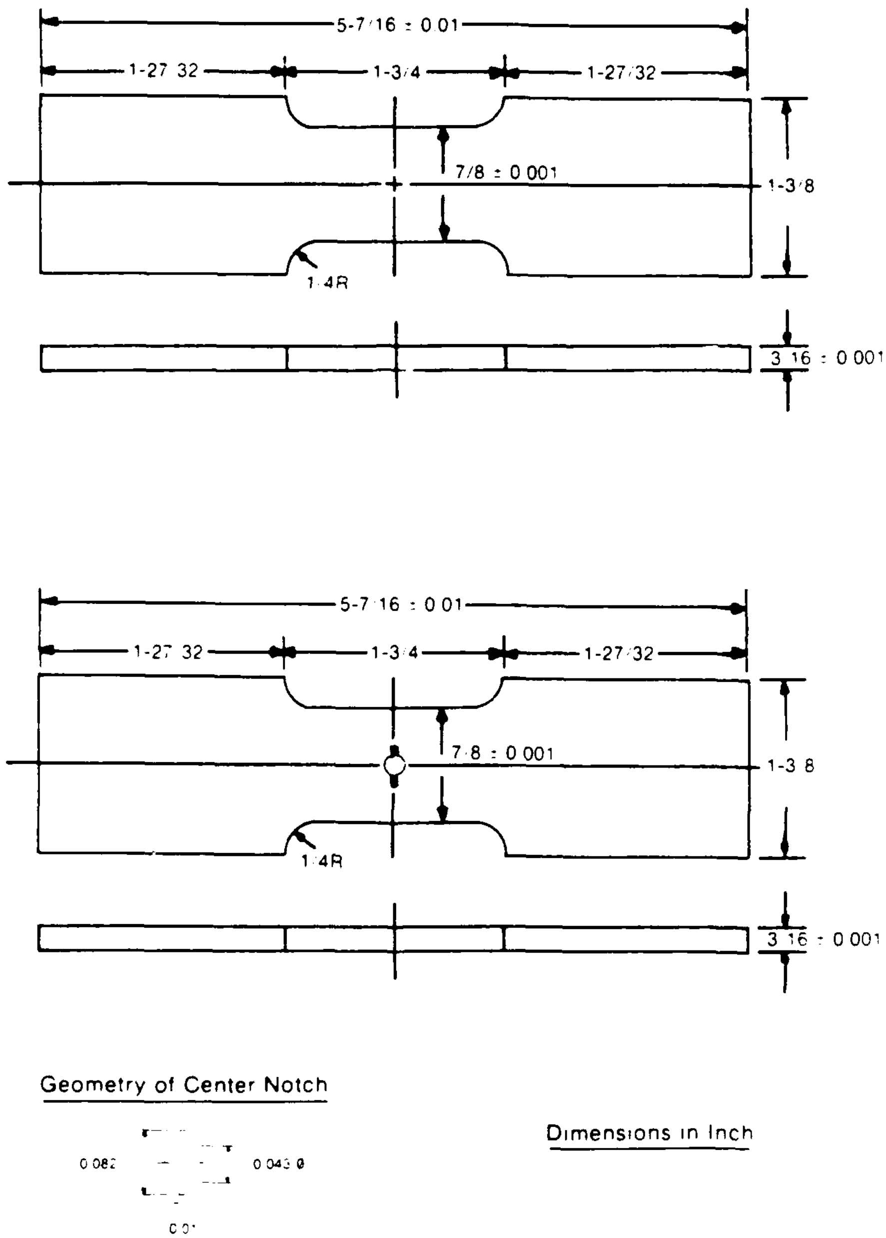

Figure 1. Specimens
(a) Rectangular Tension Test Specimen
(b) Center-Cracked-Tension Specimen for Fatigue Test

RESULTS AND DISCUSSION

The results and discussion are divided into five parts: Microstructure, Tensile Strength, Crack Growth Path, Fractography, and Fatigue Fracture Life.

MICROSTRUCTURE

The scanning electron micrographs of the specimen planes, perpendicular and parallel to the extrusion direction, are shown in Figures 2 (a) and (b), respectively. In the plane perpendicular to the extrusion direction, shown in Figure 2 (a), many white dots which are the transverse section images of SiC whiskers can be seen. In the specimen plane parallel to the extrusion direction, shown in Figure 2 (b), many white rods which are the longitudinal images of SiC whiskers are observed. Such a micrographic feature indicates that the SiC whiskers are aligned in the extrusion direction. From the micrographs, the size of the SiC whisker is measured to be between 0.1 and 1 μm dia. and 1.5 to 11 μm long. The short SiC whiskers are attributable to possible breakage during the composite fabrication process of blending, consolidation, and extrusion.

TENSILE STRENGTH

The determined ultimate tensile strength and 0.2% offset yield strength of the specimen material of LT orientation are 87.8 ksi and 83.5 ksi, respectively.

CRACK GROWTH PATH

In the tension test specimen, the crack growth path is transverse to the loading (or extrusion) direction. No significant deflection in crack growth path is noticeable, as shown in Figure 3.

In the center-cracked-tension specimen for fatigue testing, two fatigue cracks emanate initially from the two opposite tips of the center notch, shown in Figure 4. Subsequently, without appreciable growth, these cracks deflect about 100° in opposite directions and grow towards the opposite ends of the specimen, respectively. As a result, the two crack paths are parallel to each other and inclined about 10° to the longitudinal (or loading) direction. In the final overload fracture stage, the two cracks deflect transversely towards the opposite edges of the width-reduction-portions. Such a tortuous fatigue crack growth path is not changed by reducing the specimen thickness from 3/16 in. to 1/16 in. The tortuousness of the fatigue crack growth path is attributed to the alignment of SiC whiskers in the extrusion direction.

A somewhat similar deflection of the fatigue crack growth path is also observable in specimens with straight or semi-circular single edge notches, shown in Figure 5 (a) and (b).

FRACTOGRAPHY

The fractographs of a tension tested specimen are shown in Figure 6. The transverse fracture surface is entirely covered by dimples. Some of the dimples contain SiC whiskers, debonded partly or mostly, indicating microvoid nucleation at SiC whiskers. Those whiskers are fractured transversely and do not have any longitudinal crack.

The fractographs of a fatigue fractured specimen are shown in Figure 7. In the immediate vicinity of the center notch tips, numerous white dots (transverse section images of SiC whiskers) and cavities of various sizes are seen in the matrix. The dimensions of their diameters are similar to those of SiC whiskers. It appears that these cavities have been formed by those SiC whiskers which were pulled out

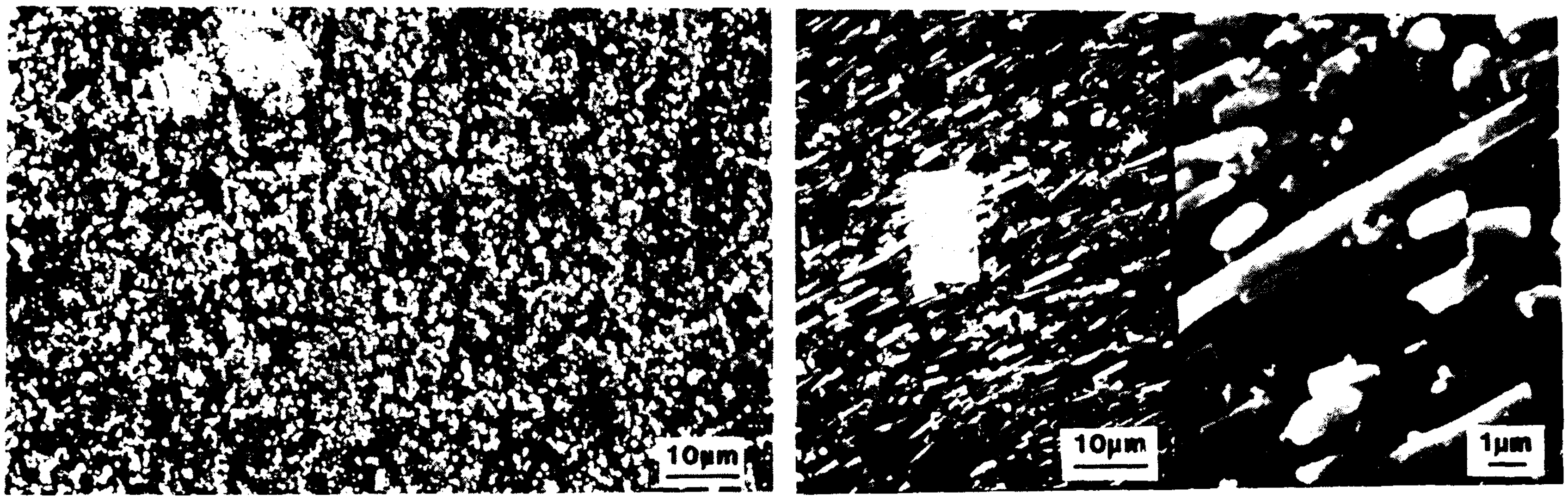

(a) (b)

Figure 2. Scanning Electron Micrographs
(a) Plane Perpendicular to Extrusion Direction
(b) Plane Parallel to Extrusion Direction

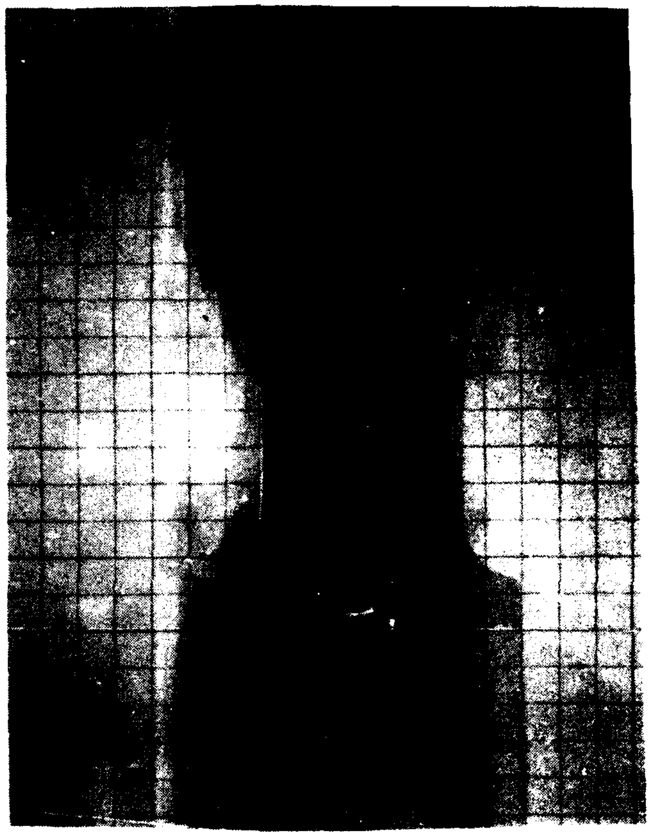

Figure 3. Crack Growth Path in Tension Test Specimen

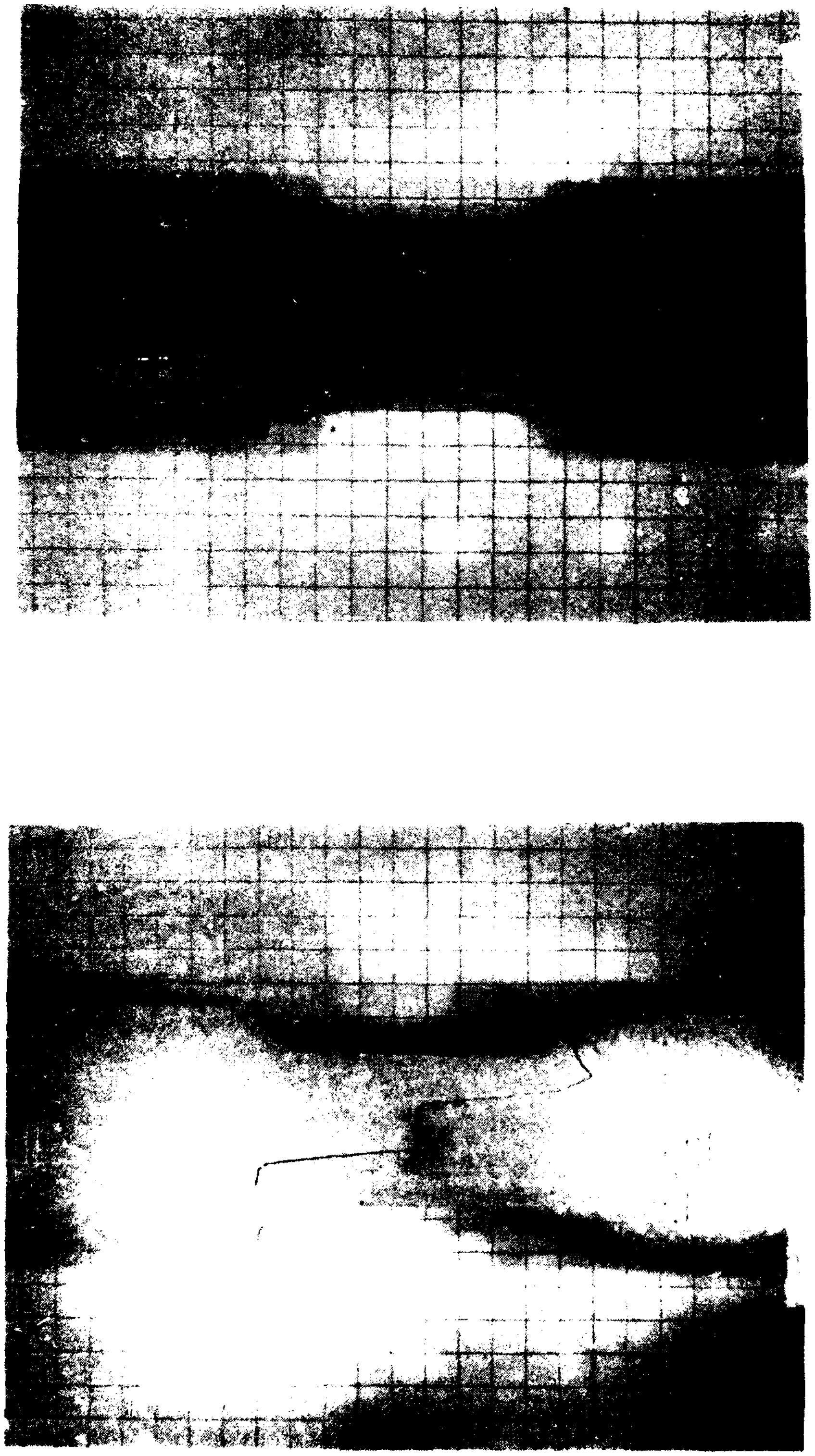

(b)

(a)

Figure 4. Fatigue Crack Growth Path in Center-Cracked-Tension Specimen
(a) Specimen Thickness: 3/16 in.
(b) Specimen Thickness: 1/16 in.

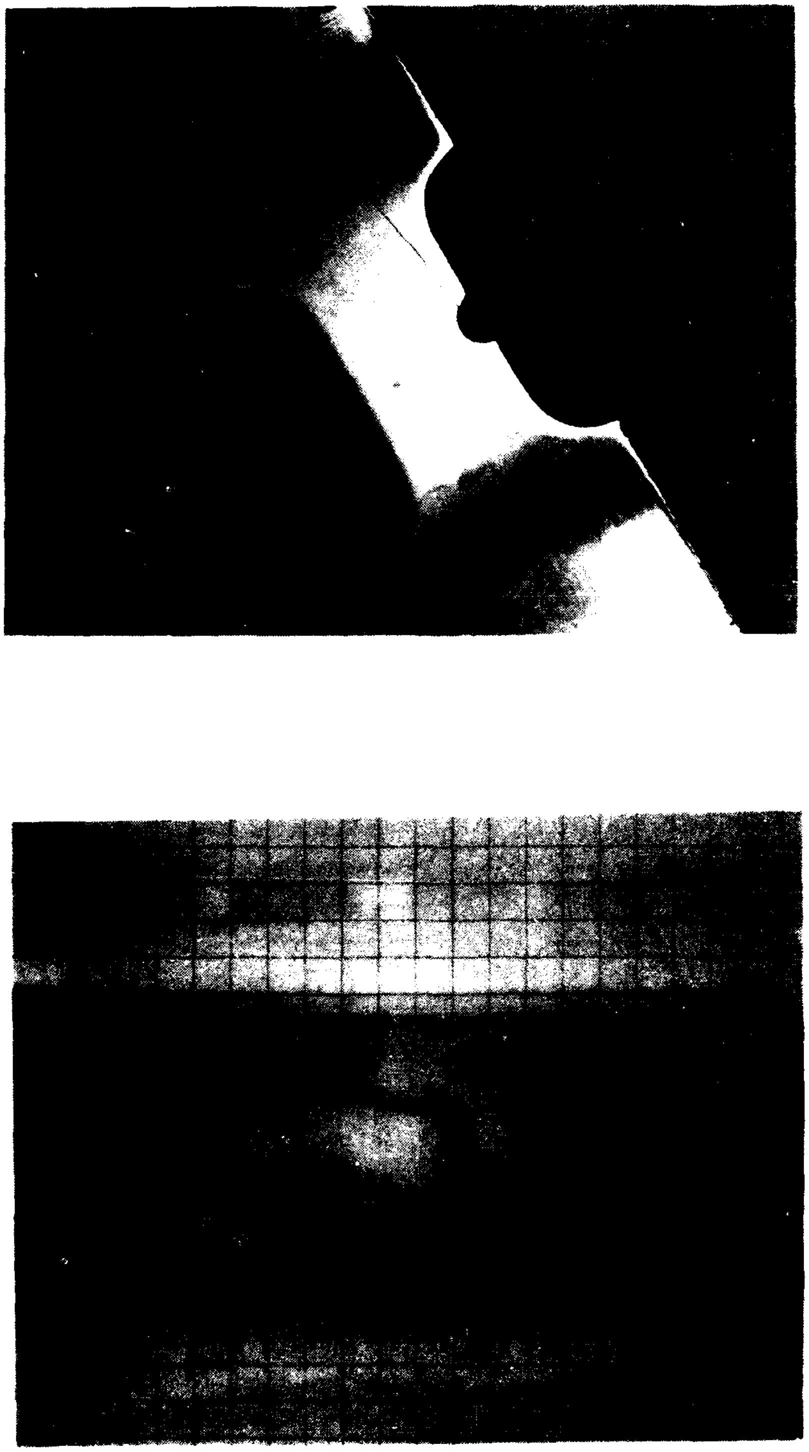

(b)

(a)

Figure 5. Fatigue Crack Growth Path in Single Edge Notch Specimen
(a) Straight Edge Notch Specimen
(b) Semi-Circular Edge Notch Specimen

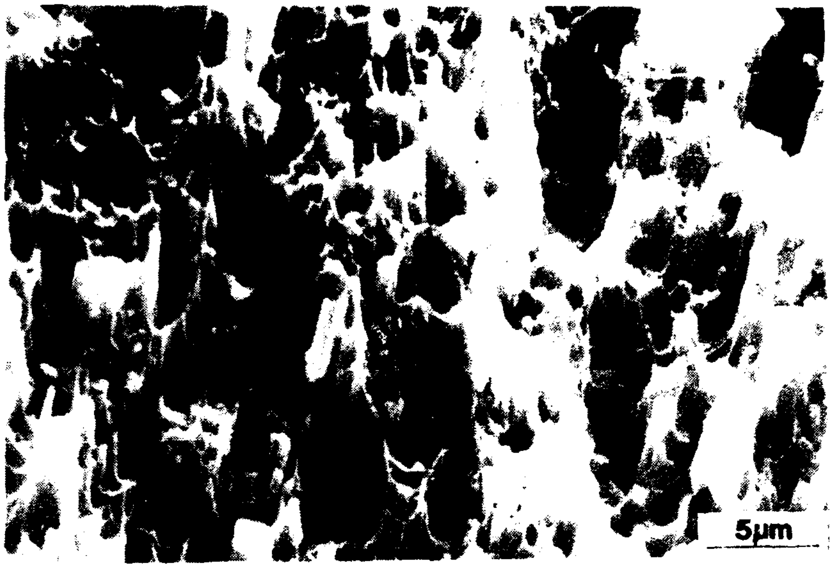

(a)

(b)

Figure 6. Fractographs of a Tension Tested Specimen

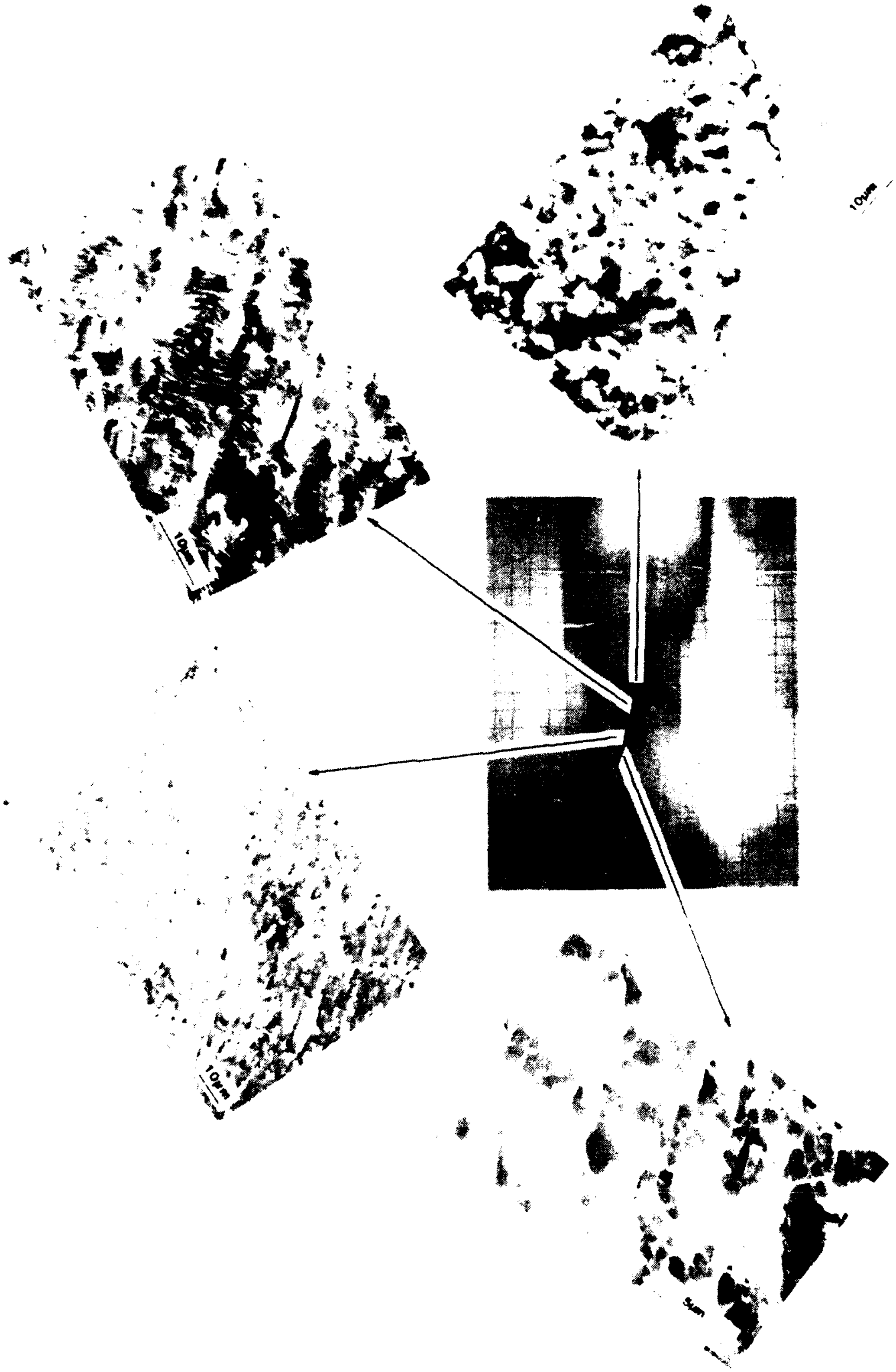

Figure 7. Fractographs of a Fatigue Fractured Specimen

during the cracking process. The matrix also shows facets and steps but no visible striation. After the deflection of the crack path to a nearly longitudinal direction, white rods (longitudinal images of SiC whiskers) and striations are visible in the matrix, indicating fatigue crack growth. Those SiC whiskers have smooth longitudinal surfaces with scattered debris-like-particles but no evidence of any cracking, Figure 8. Such a smooth longitudinal surface is probably due to debonding of the SiC whiskers during fatigue crack growth. Therefore, it is evident that the fatigue crack grows parallel to or along the longitudinal interfaces of the aligned SiC whiskers but not through them. As the crack grows further in the same direction, visible striations are fewer and fainter. Near the transverse deflection, the SiC whiskers are still seen as white rods, and dimples are present in the matrix, indicating overload fracture.

From the observed features of the crack path and the fractograph, it is apparent that:

1. During slow crack growth under fatigue loading, most of the crack path is nearly parallel to or along the longitudinal interfaces of the aligned SiC whiskers. The corresponding fractographic features are facets, steps, and striations. In this period, the maximum stress intensity factor K_{max} is less than the critical stress intensity factor of the material K_c, i.e. $K_{max} < K_c$. Accordingly for $K_{max} < K_c$, the crack grows in a direction nearly parallel to or along the longitudinal interface of the aligned SiC whiskers.

2. During the tensile fracture or the overload fracture following the slow fatigue crack growth, the crack path is transverse to the aligned SiC whiskers. The corresponding fractographic features are dimples, some of which are nucleated at SiC whiskers. In this region, $K_{max} \geq K_c$. Accordingly, for $K_{max} \geq K_c$, the crack cuts through the aligned SiC whiskers transversely.

FATIGUE FRACTURE LIFE

Due to the tortuousness of the fatigue crack growth path, it was not possible to measure the increasing crack size and define its growth rate. Consequently, only the fatigue fracture life was determined and its relationship with the applied stress range was established. A plot of stress range versus logarithm of fatigue fracture life is shown in Figure 9. The plot is a straight line and is defined by the question:

$$\Delta\sigma = 10190 - 1157 \cdot \log N_f \quad (1)$$

$$\text{or } \log N_f = 8.81 - \frac{\Delta\sigma}{1157} \quad (2)$$

where $\Delta\sigma$: stress range (psi)
N_f: fatigue fracture life (cycle)

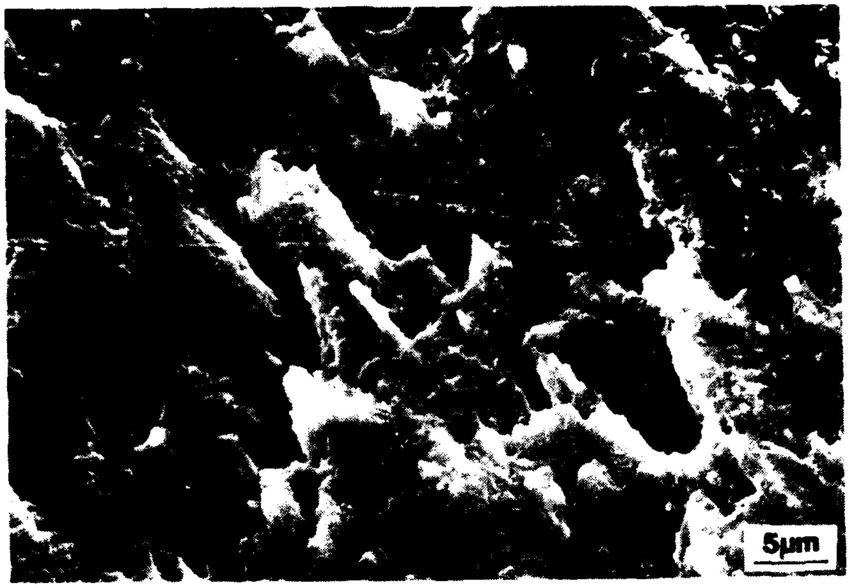

(a)

(b)

Figure 8. Morphology of a Fatigue Crack Growth Area

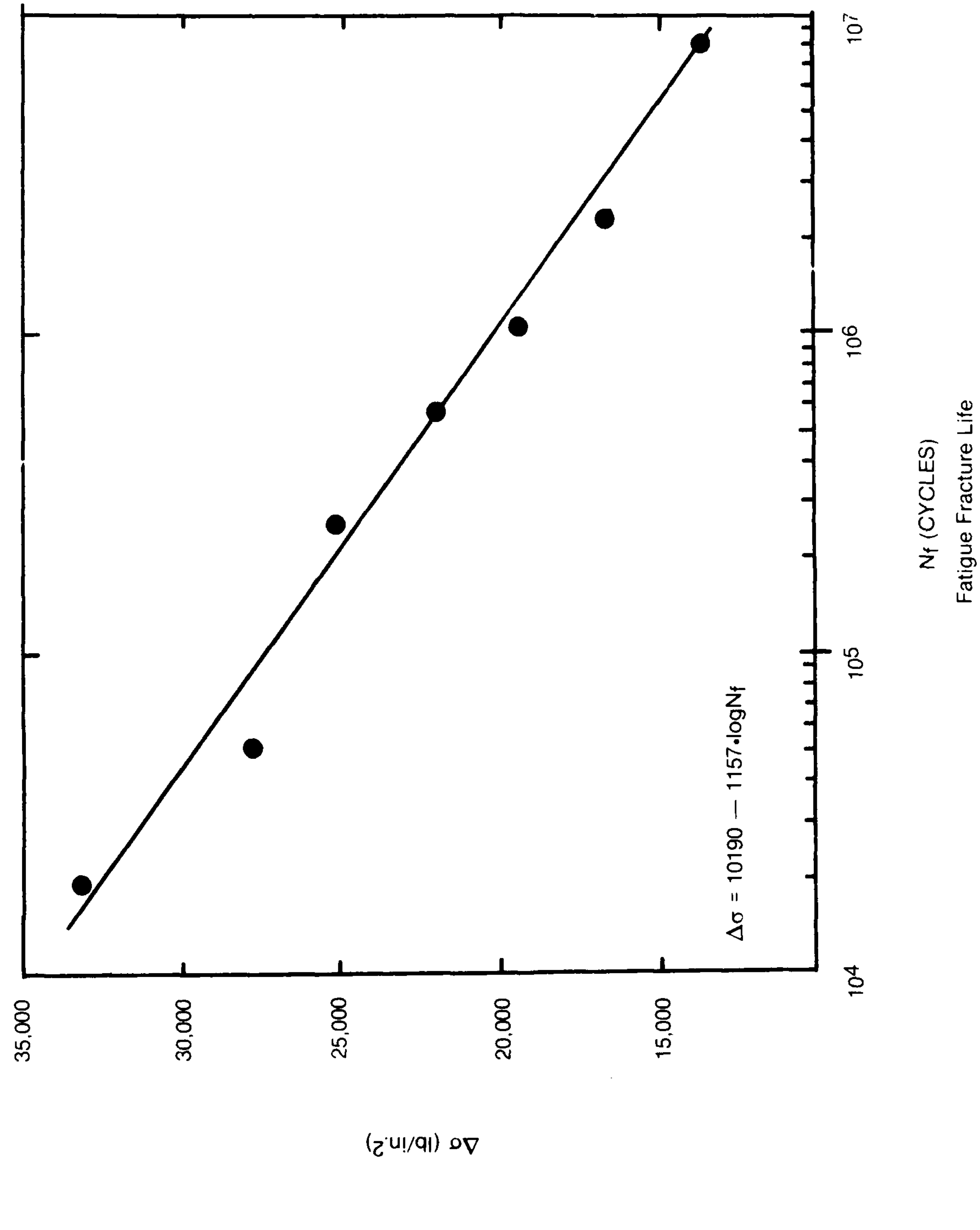

Figure 9. Variation of Fatigue Fracture Life with Stress Range

CONCLUSIONS

1. The SiC whiskers in the extruded 19.8 vol. % SiCw/2124 aluminum alloy composite are aligned in the extrusion direction.

2. During slow fatigue crack growth under the loading condition of $K_{max} < K_c$, the crack growth path is nearly parallel to or along the longitudinal interface of the aligned SiC whiskers. In this stage, fatigue striations are developed on a nearly longitudinal matrix crack plane.

3. During the tensile fracture or the overload fracture following slow fatigue crack growth under the loading condition of $K_{max} \geq K_c$, the crack growth path is transverse to the aligned SiC whiskers. In this stage, dimples are formed in the matrix.

4. The logarithm of fatigue fracture life, N_f, increases linearly with decreasing stress range, $\Delta\sigma$. This relationship is defined by the equation:

$$\log N_f = 8.81 - \frac{\Delta\sigma}{1157}$$

THIS PAGE INTENTIONALLY LEFT BLANK

REFERENCES

1. Chawla, K.K., "Composite Materials, Some Recent Development," Journal of Metals, Vol. 35, No 3, p. 82, March 1983.
2. Campbell, G.L. and Snodgrass, R.H., "Material Evaluation of Silicon Carbide Reinforced 7090 Aluminum," Final Report, Contract N6601-83-M-6355, Honeywell, Inc., Dec. 1983.
3. Wawner, F.E., "Investigation of SiC Whisker/6061 Al Composite Material Phase II: Fracture Evaluation and Hot Pressing Studies," Final Report, Contract N60921-83-M-E078, University of Virginia, Jan. 1984.
4. Arsenault, R.J., "Interfaces and Bond Strength of Silicon Carbide Aluminum Composites," in Proceedings, Sixth Annual Discontinuous Reinforced Aluminum Composites Working Group meeting 4-6 Jan. 1984, Park City, Utah, MMCIAC, Kaman Tempo, p. 1, 1984.
5. Bettadapur, S.S., "Fracture Features in 6061 Al/SiC Composites: A SEM Study," ibidem, p. 399.
6. Cox, J.M., "Fracture Behavior of 6061 Al/SiC," ibidem, p. 167.
7. Ghosh, A.K., "Investigation of Ductile Aluminum/Silicon Carbide Composites," ibidem, p. 245
8. Harrigan, W.C., "Fracture Toughness of DWL 20," ibidem, p. 211.
9. Hood, P.E., "Mechanical Properties of Forged, High-Strength, Aluminum Metal Matrix Composites," ibidem, p. 451.
10. Sanders, T.H., "TEM and SEM Analysis of SiC/Al Composites," ibidem, p. 19.
11. Crowe, C.R. and Gray, R.A., "The Effect of Notch Acuity on the Fracture Toughness of Silicon Carbide/Aluminum Metal Matrix Composites," NRL Memorandum Report 5417, Naval Research Laboratory, Feb. 27, 1985.
12. Slaughter, H.C., "Assessment of Silicon Carbide Reinforced Aluminum Composite For Aircraft Structure," Phase I Final Report, Contract N00019-81-C-0459, Jan. 1983 and Phase II Final Report, Contract N00019-82-C-0452, Lockheed-California Co., Jan. 1985.
13. Bates, W.F., "Metal Matrix Composite Structural Demonstration Program," Interim Technical Reports, Contract F33615-81-C-3211, Lockheed-Georgia Co., 1985 and 1986.
14. Papaz'an, J.M., Levy, A., and Adler, P.N., "Micro-Mechanisms of Deformation in SiC/Al Composites," Air Force Office of Scientific Research Report AFOSR-TR-87-1658, Grumman Corporate Research Center, Aug. 1987.
15. DiVecha, A.P., Crowe, C.R., and Fishman, S.G., "Properties of a SiC/Al Composite," in *Failure Mode in Composites IV*, eds., J.A. Cornie and F.W. Crossman, AIME, Warrendale, PA, 1978, p. 406.
16. DiVecha, A.P., Fishman, S.G., and Karmarkar, S.D., Journal of Metals, Vol. 33, p. 12, 1981.
17. Lederich, R.J. and Sastry, S.M.L., Mat. Sci. Eng. Vol. 55, p. 143, 1982.
18. Nieh, T.G., Met. Trans., Vol. 15A, p. 139, 1982.
19. Crowe, C.R. and Hasson, D.F., "Corrosion Fatigue of SiC/Al Metal Matrix Composites in Salt Ladened Moist Air," in Strength of Metals and Alloys, ICSMA 6, ed., R.G. Grifkins, Pergamon Press, Oxford, p. 859, 1982.
20. Arsenault, R.J., Mat. Sci. Eng., Vol. 64, p. 171, 1984.
21. DeJarnette, H.M., DiVecha, A.P., and Willard, W.A., "Fracture Toughness Measurements of Aluminum/Silicon Carbide Metal Matrix Composites," Report NSWC TR 84-20, Naval Surface Weapons Center, Jan. 1984.
22. Dolowy, J.F., Harrigan, W.C., and Webb, B.A., "Production and Characterization of Advanced Particulate-Reinforced Powder Metallurgy Products," Phase II Final Report, Contract N00024-80-C-5637, Naval Sea Systems Command, March 1983.
23. Crowe, C.R. and Gray, R.J., "The Effect of Notch Root Radius on Crack Initiation of SiC_{α}/Al" in Failure Mechanisms in High Performance Materials, eds., J.G. Early and R. Shives, Cambridge University Press, N.Y., 1984.

THIS PAGE INTENTIONALLY LEFT BLANK

DISTRIBUTION LIST (Continued)
NADC-89037-60

No. of Copies

Center for Naval Analysis 1
4401 Fort Avenue
P.O. Box 16268
Alexandria, VA 22302-0268

Advanced Composite Materials Corp. 1
Rt. 6, Box A
Greer, SC 29651

Naval Air Development Center 22
Warminster, PA 18974-5000
(20 for Code 6063)
(2 for Code 8133)

Annapolis Laboratory 1
David W. Taylor Naval Ship Research and
Development Center Detachment
Annapolis, MD 21402-1198

Naval Aviation Depot 1
Naval Air Station
Code 340
Alameda, CA 94501-5201

Naval Aviation Depot 1
Marine Corps Air Station
Code 340
Cherry Point, NC 28533-5030

Naval Aviation Depot 1
Naval Air Station
Code 340
Jacksonville, FL 32212

Naval Aviation Depot 1
Naval Air Station
Code 340
Norfolk, VA 23511-5899

Naval Aviation Depot 1
Naval Air Station
Code 340
Pensacola, FL 32508-5300

Naval Aviation Depot 1
North Island
Code 340
San Diego, CA 92135-5112

Naval Post Graduate School 1
Monterey, CA 93940
Attn: Dr. E. R. Wood (Code 67)

DISTRIBUTION LIST
NADC-89037-60

	No. of Copies
Naval Air Systems Command Washington DC 20361-3030 (2 for AIR-530) (2 for AIR-931A) (1 for AIR-5302) (1 for AIR-5304)	6
Naval Sea Systems Command Washington, DC 20362	1
Naval Air Test Center Patuxent River, MD 20670-5304	1
Naval Safety Center NAS, Norfolk, VA 23511	1
Naval Research Laboratory 4555 Overlook Ave., SW Washington, DC 20375	1
David W. Taylor Naval Ship Research and Development Center Bethesda. MD 20084-5000	1
U.S. Air Force Systems Command Wright-Patterson AFB, OH 45433 (1 for FBR) (1 for FB) (1 for LLD) (1 for FYA) (1 for LAM) (1 for FBA) (1 for LPH)	7
Chief of Naval Research 800 N. Quincy ST Arlington, VA 22217-5000	1
Defense Technical Information Center ATTN: DTIC-FDAB Cameron Station BG5 Alexandria, VA 22304-6145	2